Department of the Navy
Bureau of Ordnance
Contract NOrd-9612

A SCALE MODEL INVESTIGATION OF THE EFFECT OF JET CONFIGURATION ON SKIN FRICTION FOR THE MK-40 TORPEDO

R. L. Waid

Hydrodynamics Laboratory
California Institute of Technology
Pasadena, California

Report No. E-12.6
September 1952

John T. McGraw
Project Supervisor

Copy No. 55

CONTENTS

ABSTRACT

An analytical study, combining jet diffusion patterns and jet velocities, indicates that there are four methods of eliminating the clinging jet phenomenon which occurs on the Mk-40 Torpedo Test Vehicle. It is shown that extension of the nozzles along the existing nozzle axis appears to present the simplest method of design improvement. Experiments were conducted on a modified model of the Mk-40 to verify the analysis. It was found that for the operational jet-to-model velocity ratio, (U/V) of 2, a nozzle extension of 6 nozzle diameters is the minimum required to provide cling-free performance. All experiments and calculations were made for the case of a body without exhaust ports or gas discharge.

INTRODUCTION

The jet configuration on the present Mk-40 Torpedo Test Vehicle presents a complex combination of jet diffusion and nonparallel flow. Unpublished tests in the High Speed Water Tunnel at the California Institute of Technology, and tests at the Experimental Towing Tank, Stevens Institute of Technology[1]* showed a marked increase in drag at low jet-to-free-stream velocity ratios, U/V, near the operational velocity ratio of 2. This study was conducted to investigate a means of eliminating this increase in drag.

The experimental work in the High Speed Water Tunnel was preceded by semi-empirical calculations to investigate possible causes and remedies for the drag increase. It is believed that the high velocity jet which originally discharged from below the surface of the body does not flow free of the torpedo but clings to (or "scrubs") the entire afterbody. This behavior could be expected to alter the form drag and increase the friction drag of the body.

In order to simplify the calculations and experiments, the effect of gaseous exhaust was neglected, although it is realized that it may have considerable effect.

---

*See bibliography on page 20.

CALCULATION OF THE TRAJECTORY OF A JET DIFFUSING INTO AN AMBIENT STREAM AT A SMALL ANGLE

This approximate analysis is based on the experimental data of Küchemann[2] and of Albertson, Dai, Jensen and Rouse[3]. Since the latter report deals only with jet diffusion into a fluid which is initially at rest, it was used mainly as a comparison with the Küchemann data. Both of these experiments were conducted with three-dimensional air jets, and they covered a wide Reynolds number range without severe flow variations. Accordingly, it is assumed that the test results are also applicable to the water jets studied here.

Küchemann conducted experiments on an air jet of 70 millimeters in diameter with its axis parallel to the free-stream or ambient velocity. The jet discharged in the downstream direction with jet velocities of 33, 44, and 66 meters/sec for ambient velocities of 0, 11, and 33 meters/sec, respectively. In applying the Küchemann data to the case where the jet axis is not parallel to the free stream, only kinematical relationships will be utilized. Flow velocities due to the jet are superimposed on the flow that would exist if the jet were absent. The dynamical requirements are assumed to be approximated in the employment of the experimental data. The sole justification for this linearization of the turbulent diffusion problem will be found in the fair agreement between the calculations and the experimental observations.

Properties of a Diffusing Jet in a Parallel Ambient Stream

This section deals with the simple case of a diffusing jet which issues parallel to an ambient stream. The properties presented here will be utilized in the following section for the analysis of a jet which issues at an angle into an ambient stream.

By studying the velocity profiles at right angles to the jet axis and downstream from the nozzle, some useful properties can be established. Figure 1a represents one of these profiles. Only the axial velocity components will be studied here. The effect of any radial components will be assumed to be negligible. The X-axis is chosen parallel to the jet axis and to the ambient stream. The Y-axis is then normal to direction of flow. The center of the coordinate system is set at the center of the jet nozzle opening.

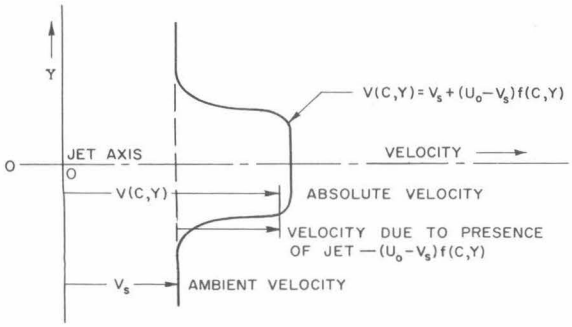

Fig. 1 a - A typical velocity profile of a jet diffusing into a parallel ambient stream

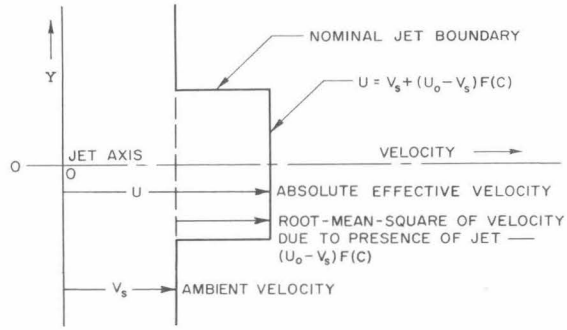

Fig. 1 b - A rectangular velocity profile representing the typical velocity profile shown in Fig. 1 a

The absolute velocity, V(X, Y), parallel to the X-axis is a function of both X and Y. It is composed of two components. One component is the ambient stream velocity parallel to the jet axis, V_s, which is a constant or independent of position. The other component is the relative velocity of the jet with respect to the stream and is dependent upon position. It is a function of the distance from the jet nozzle and the distance from the jet axis, and can be expressed as $(U_o - V_s)\, f(X, Y)$ where U_o is the initial velocity of the jet at the nozzle. For a fixed distance, C, from the jet nozzle, the preceding expression becomes $(U_o - V_s)\, f\,(C, Y)$. The absolute velocity at this given distance from the nozzle, V(C, Y), is the sum of the two components,

$$V(C, Y) = V_s + (U_o - V_s)\, f(C, Y) \quad . \qquad (1)$$

Since only that portion of the absolute velocity which exceeds the ambient velocity is caused by the presence of the jet, this part of the absolute velocity is distinctive of the jet. To simplify the later analysis, the actual jet velocity profile will be replaced by a rectangular profile, as seen in Fig. 1 b. This step function will be bounded on the sides by the nominal boundaries of the jet. The boundary will be arbitrarily selected so as to enclose the region in which the presence of the jet causes a significant change from the jet-free ambient stream conditions. In the report by Albertson, Dai, Jensen and Rouse, the nominal boundary is taken to be the loci of all axial velocity components which are approximately 6 percent of the respective centerline velocities. This criterion was applied

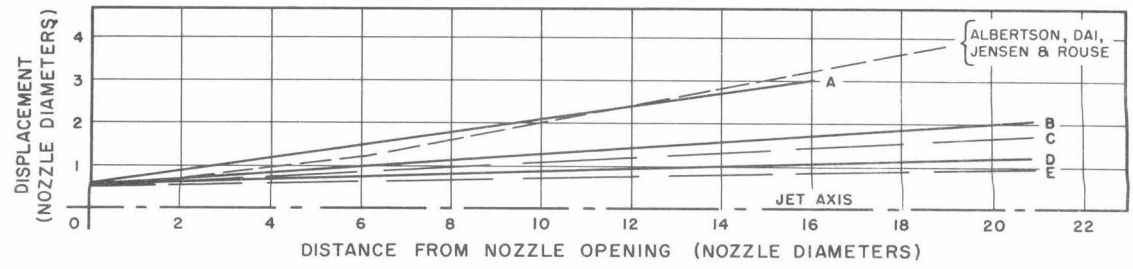

Fig. 2 - The nominal boundary of a diffusing jet as a function of distance from the nozzle opening for several jet-to-ambient velocity ratios. These curves are for the same respective conditions as Fig. 3.

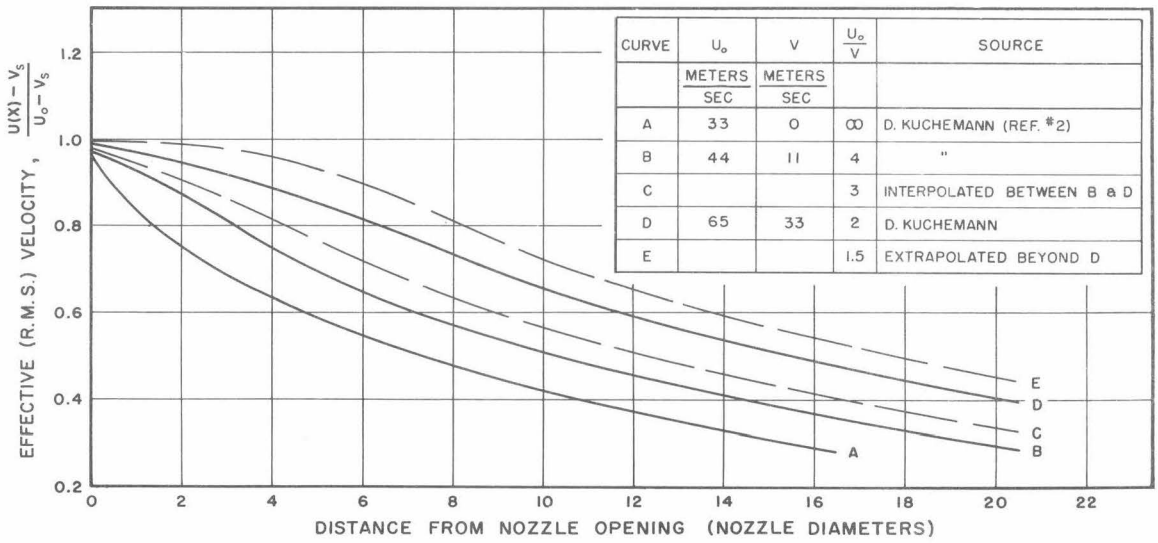

CURVE	U_o METERS/SEC	V METERS/SEC	$\frac{U_o}{V}$	SOURCE
A	33	0	∞	D. KUCHEMANN (REF. #2)
B	44	11	4	"
C			3	INTERPOLATED BETWEEN B & D
D	65	33	2	D. KUCHEMANN
E			1.5	EXTRAPOLATED BEYOND D

Fig. 3 - Effective or root-mean-square velocity of a diffusing jet as a function of the distance from the nozzle opening for several jet-to-ambient velocity ratios.

to the Kuchemann data, Fig. 2. The curves show the nominal jet boundaries for several jet and ambient stream velocities.

The magnitude of the step function will be taken to be the effective or root-mean-square of the respective typical velocity profile. This velocity component can be expressed as $(U_o - V_s)\, F(X)$. The new term, $F(X)$, is actually a constant for a given distance, $X = C$, from the jet nozzle, and is equal to the root-mean-square of the typical velocity profile within the nominal jet boundaries.

The absolute velocity, U(X), of the jet with the step function profile is a constant for any given distance, X, from the nozzle and is given by

$$U(X) = V_s + (U_o - V_s)\, F(X) \quad . \tag{2}$$

This equation can be rewritten in the following form:

$$\frac{U(X) - V_s}{U_o - V_s} = F(X) \quad . \tag{3}$$

Effective jet velocities were calculated from the Küchemann data and the curves in Fig. 3 were plotted. This graph thus provides an empirical evaluation of the F(X) from Eq. (3).

Extension of Calculations to the Case of a Jet Diffusing into an Ambient Stream at a Small Angle

This section deals with the analysis of the more complex diffusion problem of a jet which issues into a stream at a small angle. An analysis of this situation would normally be expected to involve a study of the flow, the momentum, and the energy of the jet and of the ambient fluid. Since in this study we are interested only in the nominal boundaries of the diffusing jet, the approach can be greatly simplified. By limiting the discussion to small angles, the effect of the nonparallel flows on the diffusing jet will be kept to a minimum. The nominal boundaries of the jet will be assumed to remain symmetrical about the jet centerline and to have the same displacement as in the simple case of a parallel efflux. Thus, it is assumed that the problem involving the flow, the momentum and the energy is approximated by using the experimental data obtained from the Küchemann report. The following considerations deal with a lateral movement of the jet boundaries which is due to the small normal velocity components of the ambient stream.

Taking the velocity components which are parallel to the jet axis results in a configuration which is identical to the simple case studied in the previous section (note Fig. 1 a) with the X-and Y-axis parallel and normal to the jet nozzle axis. If it is assumed that the step function representation is still valid, the absolute velocity of the jet parallel to the jet axis is still represented by U(X) as in Eq. (2). The components in the X, Y

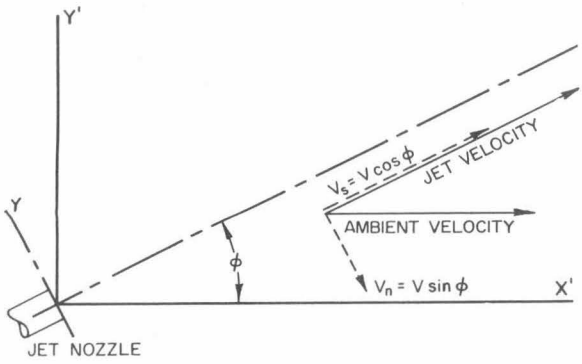

Fig. 4 - Velocity components produced by a jet which diffuses into an ambient stream at an angle

coordinate system above can be resolved into an X'- and Y'-coordinate system which has the same origin but is parallel and normal to the ambient stream, Fig. 4. Using these components, the jet trajectory can be studied in the X'- and Y'-coordinate system.

Taking U(X) from Eq. (2), the resultant velocity component normal to the ambient stream, v_y', is as follows:

$$v_y' = \frac{dy'}{dt} = U(X) \sin \phi - V_N \cos \phi \ . \tag{4}$$

The component parallel to the ambient stream, v_x', is

$$v_x' = \frac{dx'}{dt} = U(X) \cos \phi + V_N \sin \phi \ . \tag{5}$$

Division of Eq. (4) by Eq. (5) results in the slope of the trajectory of any particle in the jet stream,

$$\frac{dy'}{dx'} = \frac{U(X) \sin \phi - V_N \cos \phi}{U(X) \cos \phi + V_N \sin \phi} \ . \tag{6}$$

Substituting Eq. (2) into Eq. (6) and simplifying, yields the following equation:

$$\frac{dy'}{dx'} = \tan \phi \ \frac{F(X)}{F(X) + \dfrac{\tan^2 \phi + 1}{\dfrac{V_o}{V_s} - 1}} \tag{7}$$

For the small angles involved, the term F(X) can be approximated by F(x'). Integrating yields:

$$y' = \tan \phi \int_o^a \frac{F(x')}{F(x') + B} \, dx' \qquad (8)$$

where

$$B = \frac{\tan^2 \phi + 1}{\frac{V_o}{V \cos \phi} - 1}$$

$$F(X) \approx F(x')$$

Since the jet boundaries and the function of (X) are not easily expressed mathematically, the above integration can be treated graphically. After the trajectory has been established the nominal boundaries of the jet can be applied using the derived trajectory as the jet centerline. Figure 5 shows the results of this analysis for several jet-to-ambient velocity ratios and for several jet-to-ambient velocity angles.

Comparison with Experimental Jets

Figure 6 shows the jet boundary as observed during several experimental tests on a modified model of the Mk-40 as compared with the predicted nominal jet boundary using the above analysis. The two jets compare quite favorably up to 8 nozzle diameters from the nozzle. Beyond this point the experimental jet boundary turns toward the free-stream direction more rapidly than does the predicted jet. This could be explained by the fact that the experimental jet was in such a position as to allow interference from the flow of the free stream around the three-dimensional test body. For this particular velocity ratio, the data is quite meager in the region beyond 8 nozzle diameters, consequently limiting the applicability of the data. Thus, it appears that this approximate analysis of a jet diffusing into a free stream at a small angle provides a fair indication of the actual jet pattern on the model.

Application to Mk-40 Torpedo Model

The first assumption in the analysis required a uniform parallel flow in the free stream. The pressure distribution over the section of the body

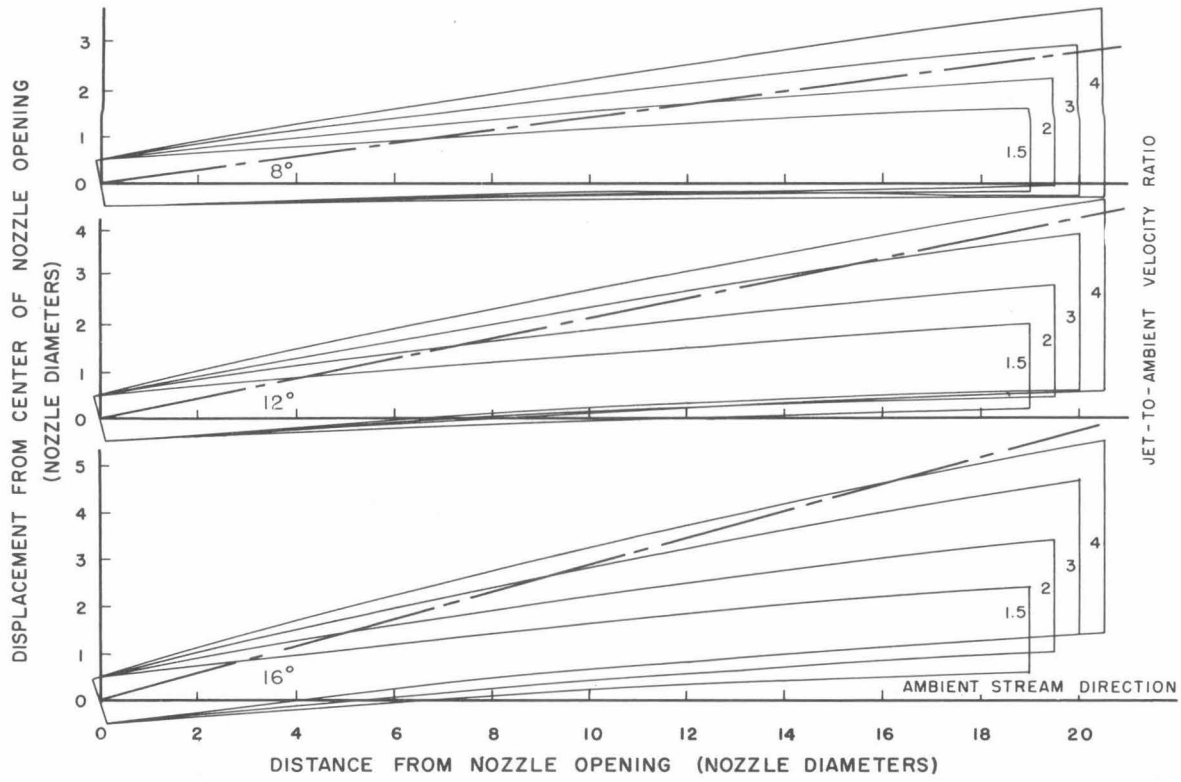

Fig. 5 - Calculated nominal jet boundaries for jets diffusing into an ambient stream at angles of 8, 12, and 16° for jet-to-ambient stream velocity ratios of 1.5, 2, 3, and 4

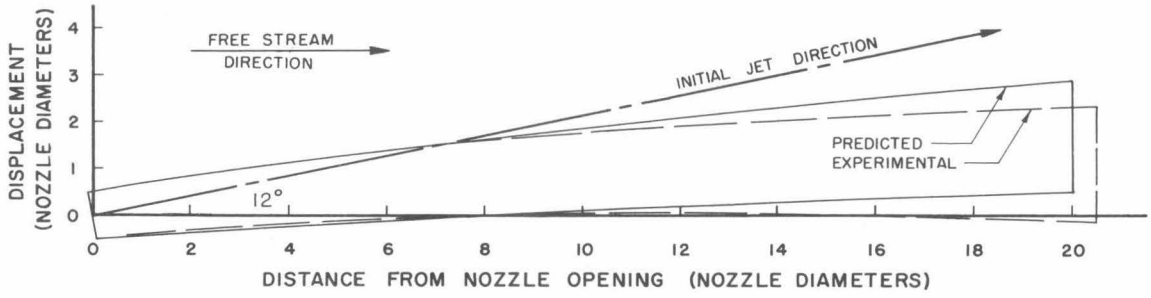

Fig. 6 - Comparison of the experimental jet boundary with the predicted boundary for a jet-to-free stream velocity ratio of 2:1 and an angle of 12°

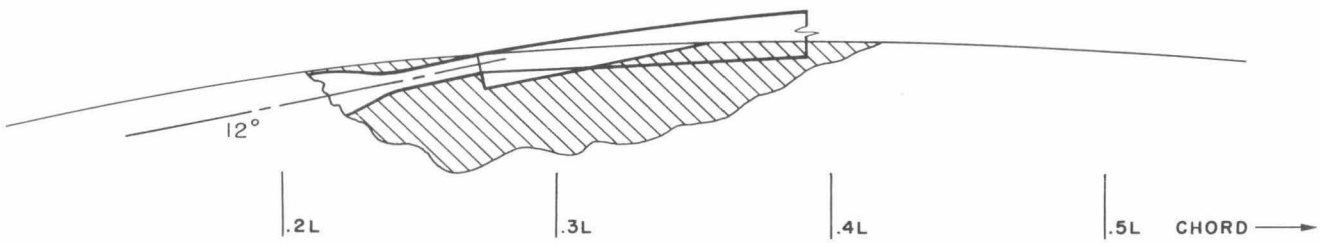

Fig. 7 - Sketch of the original Mk-40 Torpedo Test Vehicle jet configuration with the analytically determined jet boundary superimposed. U/V = 2

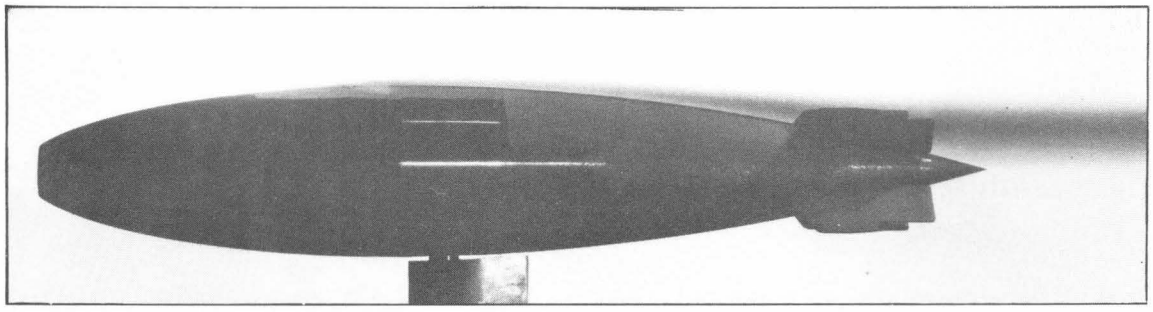

Fig. 8 - Photograph of a 2-in. diameter model of the Mk-40 torpedo operating in the High Speed Water Tunnel at a jet velocity of 60 fps and a tunnel velocity of 30 fps

of the Mk-40 where the jet nozzles break the surface is quite flat, indicating a uniform axial velocity distribution. Although velocity actually decreases away from the surface, the jet does not extend very far above the body surface, as can be seen in Fig. 7. The body contour has a large radius of curvature in this region, causing near parallel flow. Just beyond the 40 per cent point of the body, the curvature becomes greater and the pressure distribution changes, limiting the range of applicability of the analysis. Figure 7 shows the original Mk-40 jet configuration with a predicted jet at a U/V of 2. It is quite apparent that the jet does not leave the body as a free jet. The relief penetrates very nearly to the centerline of the jet, causing rapid diffusion at this point. Hence the effectiveness of the jet in penetrating the free stream is greatly diminished, causing the jet to be carried with the free stream flow lines, as can be observed in Fig. 8. This picture is of a 2-in. diameter model of the Mk-40 as it was tested in the High Speed Water Tunnel at a jet velocity of 60 fps and a tunnel velocity of 30 fps. The jet is

seen to cling to the afterbody for 30 percent of the model length and then only to separate a very small amount. High velocity flow is thus present over the aft 70 percent of the model, obviously increasing the drag due to skin friction. This illustrates why it is desirable to eliminate the scrubbing phenomenon.

Methods to Eliminate Scrubbing Based on Results of Simplified Calculations

1. Deepening and elongating the relief below the nozzle would keep the jet from striking the relief and eliminate unnecessary diffusion. The effect of a modification of this type cannot be calculated as described above. The flow in and around this groove would tend to turn the main jet further towards the body than the analysis would indicate. Hence, a relief would have to extend over at least the center 30 percent of the body. This would create a very large irregularity in the body contour and would increase the form drag significantly. The probable minimum design for this method is illustrated in Fig. 9 a.

2. Moving the nozzle laterally above the body surface could free the jet entirely from the afterbody. This method is not practicable because of the interference that would occur between the large diameter prenozzle passages and the desired nose contour. The minimum design to eliminate scrubbing, shown in Fig. 9 b, places the nozzle opening entirely above the body contour.

3. Changing the diverging angle of the jet axis a few degrees might free it from the relief. Using the calculations based on a 16° angle from the model axis (as compared to 12° for the Mk-40) the present configuration would still scrub. In addition, there would be a 1.8 percent loss in useful propulsion because of the decreased axial component of thrust. The minimum scrub-free design combining this method and the following one is shown in Fig. 9 c.

4. Extending the present nozzle along the axis of the nozzle seems to be the most practical approach. Superimposing the previously developed jet pattern at various nozzle elongations indicates that scrubbing could be eliminated without an excessive surface disturbance. Extending the nozzle 6 nozzle diameters along the axis should free the jet entirely from the relief and the afterbody, as shown in Fig. 9 d. Any shorter extension than this might still cause scrubbing.

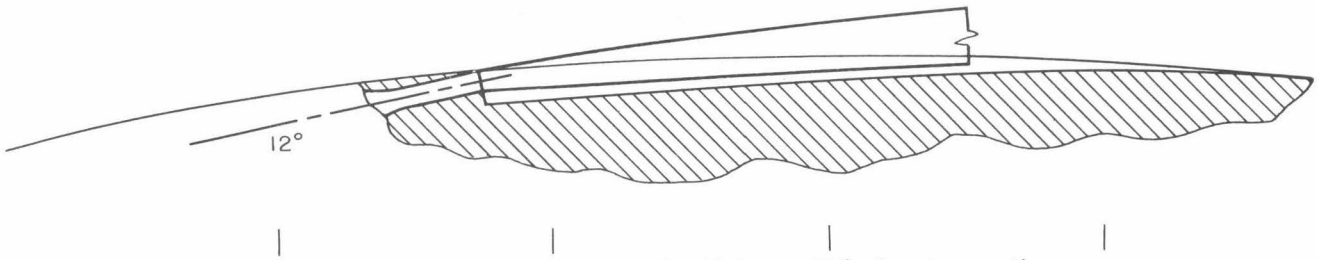

a. Deepening and elongation of relief over 30% of center section

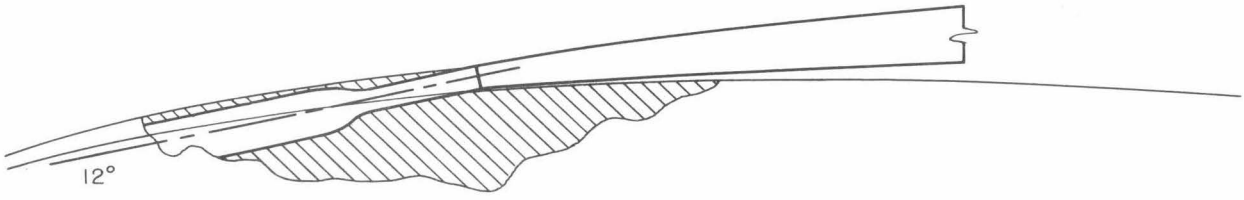

b. Lateral extension of one nozzle diameter above original position

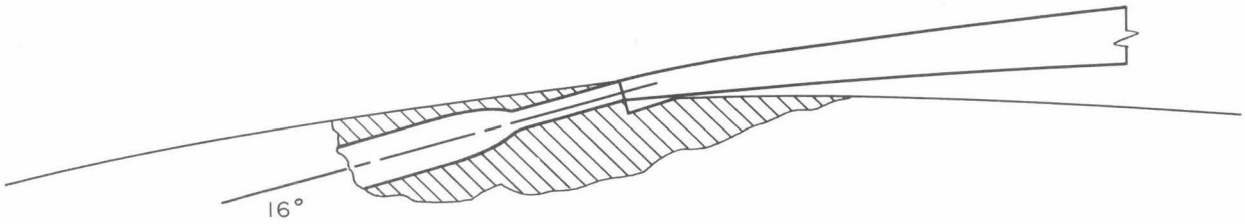

c. Increase diverging angle of nozzle axis from 12° (original) to 16° (causes 1.8% loss of useful propulsion)

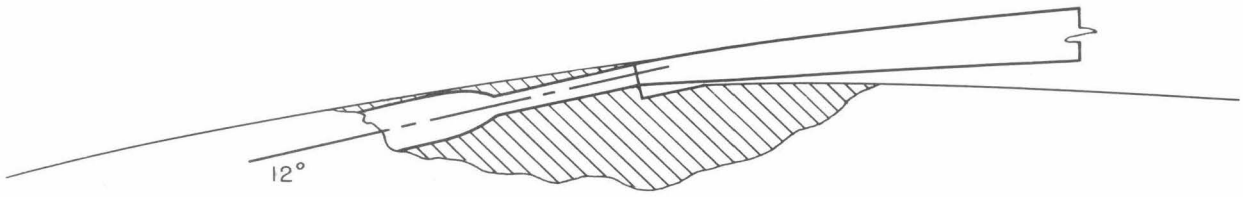

d. Six diameter extension of nozzle along original axis

Fig. 9 - Several predicted minimum design modifications for the elimination of the clinging jet at U/V = 2

EXPERIMENTAL INVESTIGATION

The simplified calculations show that several approaches can be made to the elimination of the scrubbing phenomena. The method of extending the nozzles was used for the series of tests made in the High Speed Water Tunnel.

Experimental Method

A 2-in. diameter model of the Mk-40 Test Vehicle was modified by sealing all but one of the jets and extending that one 14 nozzle diameters from its original position. The jet was fed from an exterior source which was calibrated with an orifice meter. A small accumulator loaded with a saturated solution of potassium permanganate was tapped into the intake of the orifice meter. Small shots from this accumulator provided the dye for coloring the jet so that it could be photographed. The model was rigidly mounted, so consequently no drag data are available. This preliminary study was to investigate the feasibility of this type of approach in expectation of later drag studies. The model was operated at various jet velocities and the tunnel velocity was varied to get the desired velocity ratios. The nozzle was cut off successively until it was of the original configuration.

Photographs were taken of the colored jet at a series of nozzle lengths for a series of jet-to-tunnel velocity ratios. Analysis of the photographs was made into the following four major classifications:

1. The jet was completely free from the surface of the model, as in Fig. 10 a.

2. The major part of the jet was free, but there was some diffusion toward the surface that indicated light scrubbing, as in Fig. 10 b.

3. The major part of the jet was diffusing toward the surface, causing moderate scrubbing, as shown in Fig. 10 c.

4. The major part of the jet was completely scrubbing over some portion of the surface, as seen in Fig. 10 d.

A combined analysis of nozzle extension and U/V effect on the Mk-40 scrubbing phenomena is shown in Fig. 10.

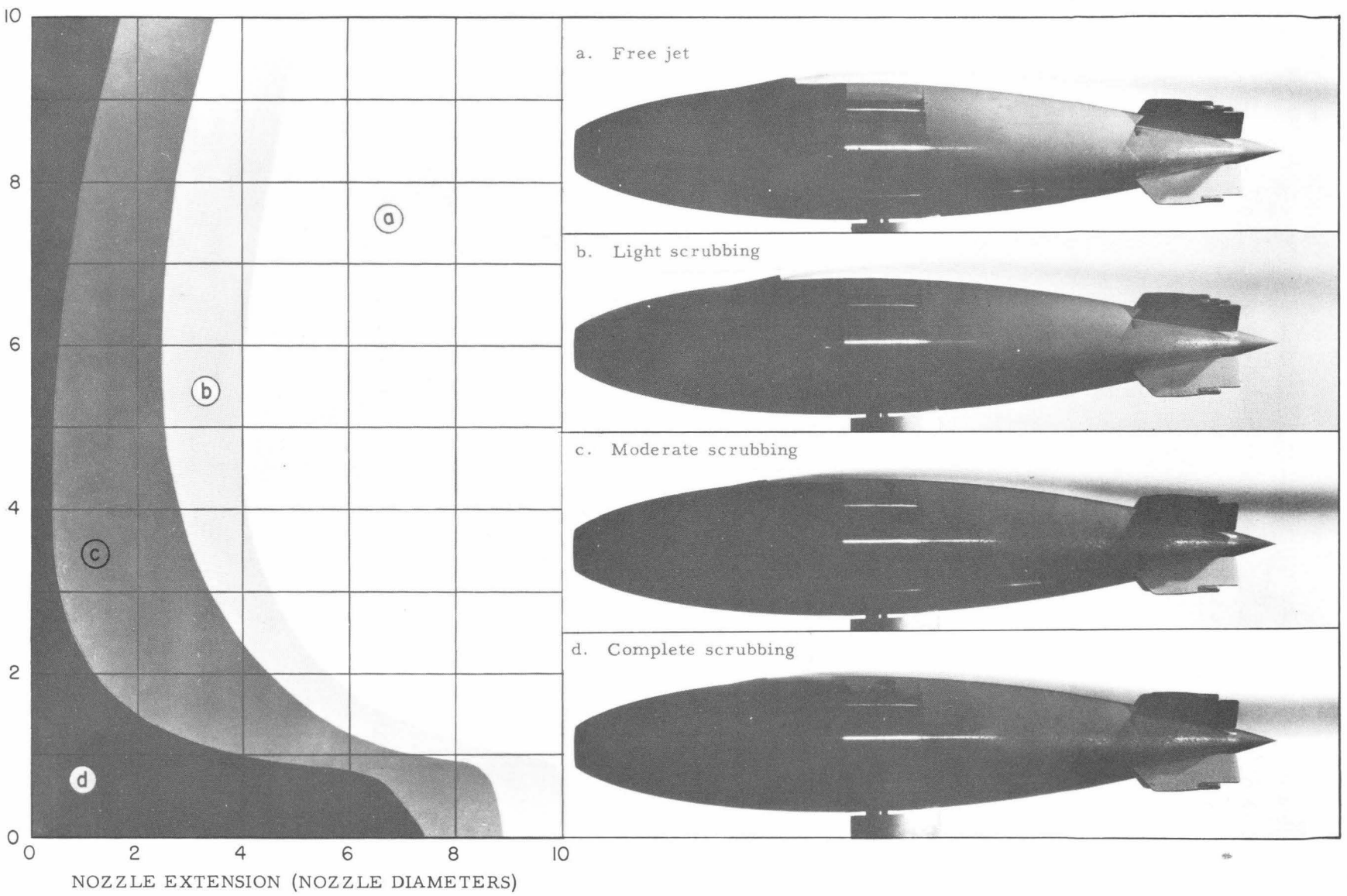

Fig. 10 - Results of photographic study of scrubbing on a modified 2-in. diameter model of the Mk-40 Torpedo Test Vehicle

Discussion of Results on a Modified Model Mk-40

At low U/V ratios (1 or less) complete scrubbing occurs with nozzle extensions up to 6 diameters. The free stream velocity is equal to or greater than the jet velocity, causing the jet to follow the body contour. The normal jet diffusion adds to this effect to cause scrubbing over considerable portions of the afterbody, Fig. 11a - b. Around 6 diameters extension the nozzle opening is completely above the body surface and the jet then is carried aft at a definite distance from the surface, causing only a moderate amount of scrubbing due to normal jet diffusion, Fig. 11 c. Extensions of 10 to 14 diameters place the jet far enough from the surface so that the diffusion itself does not affect the afterbody, as shown in Fig. 11 e.

At a higher U/V ratio, the jet has a relatively larger component normal to the body which forces it further into the flow before it is turned downstream, Fig. 12 a - c. If the clearance is great enough, the normal jet boundary will be clear of the surface, as shown in Fig. 12 d. Since the normal diffusion of the jet increases with increased U/V, a high velocity ratio causes the jet to broaden more than it is shifted away from the surface, so that scrubbing will then occur even with an increased U/V, Fig. 12 e.

As can be seen in Fig. 10, the original configuration is so situated that complete scrubbing occurs at all U/V ratios.

Results as Applied to the Operational Mk-40

U/V ratios of 1.85 to 2 represent the operating range of the Mk-40 Test Vehicle. As shown in Fig. 10, the minimum nozzle extension for scrub-free operation of the jet is 6 nozzle diameters. It is significant to note that this particular extension places the nozzle opening completely above the body surface. This is the same as the minimum design for a lateral extension of the nozzle. Hence, it appears that at the low U/V ratios that are used, the jet cannot be submerged below the smooth body contour.

Figure 13 shows the Mk-40 model at operational U/V = 2 for nozzle extensions of 0, 2, 4, 6, and 8 diameters.

The contouring of the outside of the nozzle extension was not elaborate since only the effect of jet flow was being investigated. Since the experimental runs (see Appendix) show no difference between the contoured

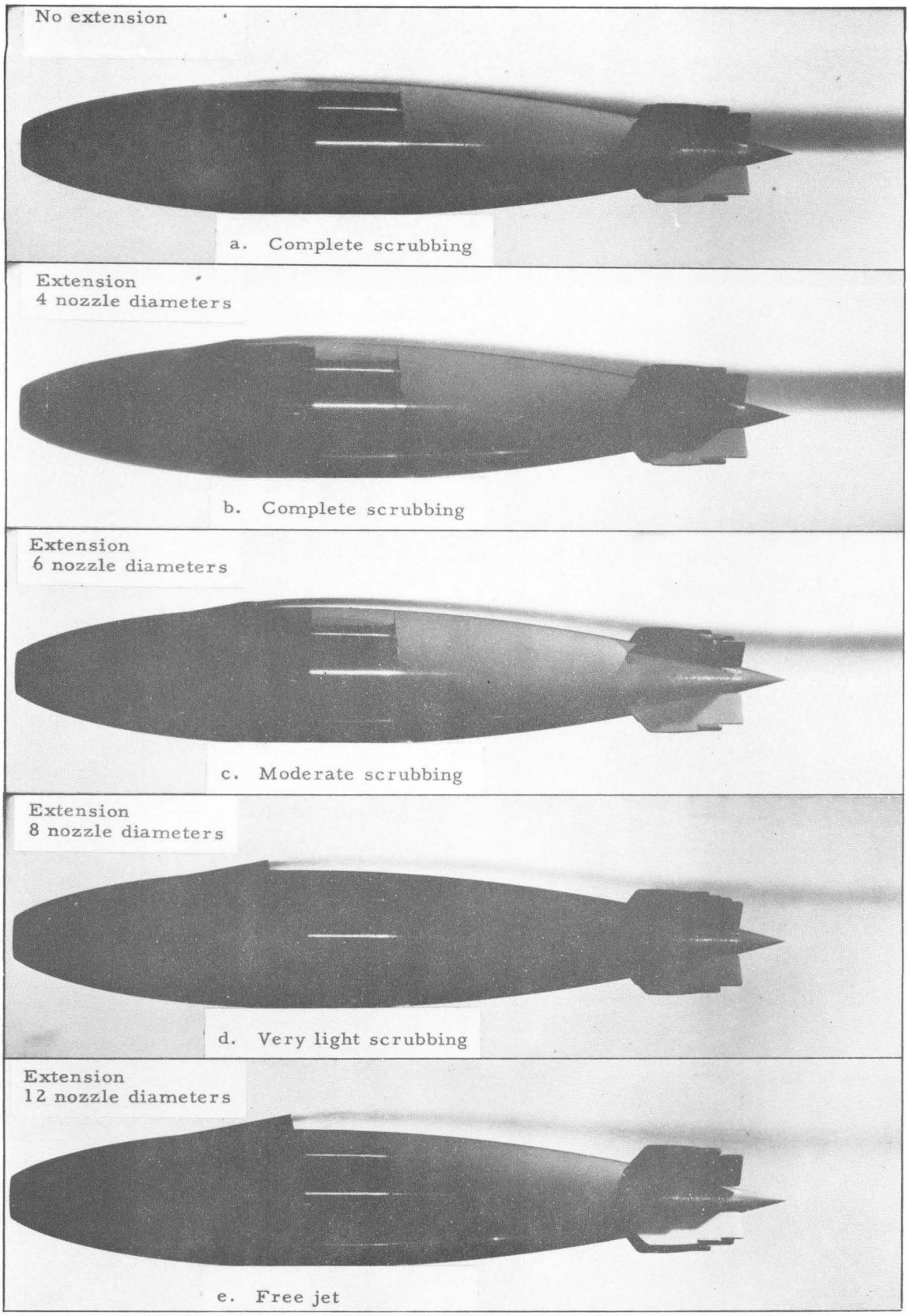

Fig. 11 - Photographs of modified Mk-40 model at low jet-to-model velocity ratio (U/V = 1) showing effect of nozzle extension

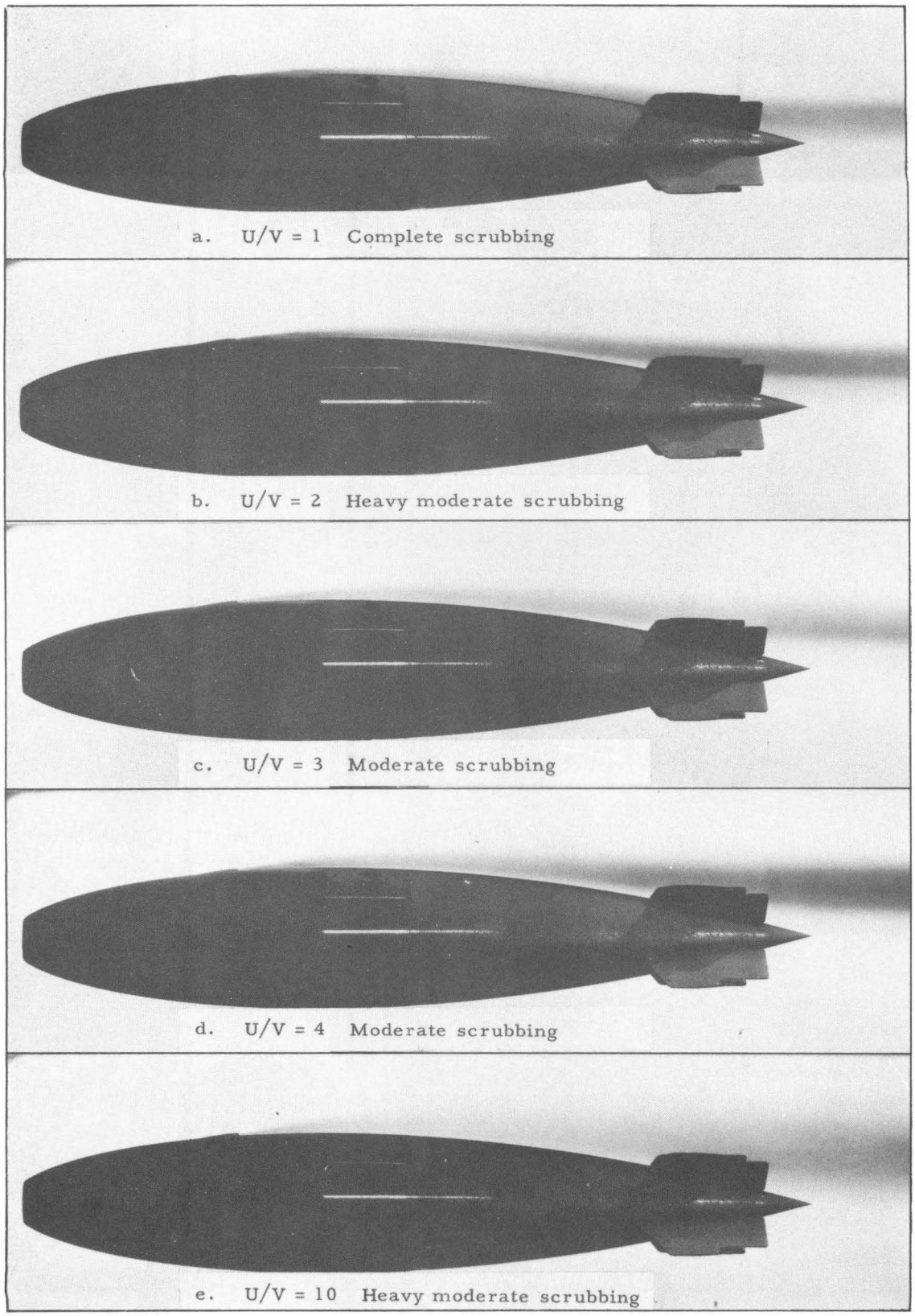

Fig. 12 - Photographs of modified Mk-40 model showing effect of U/V on scrubbing for a nozzle extension of 2 diameters

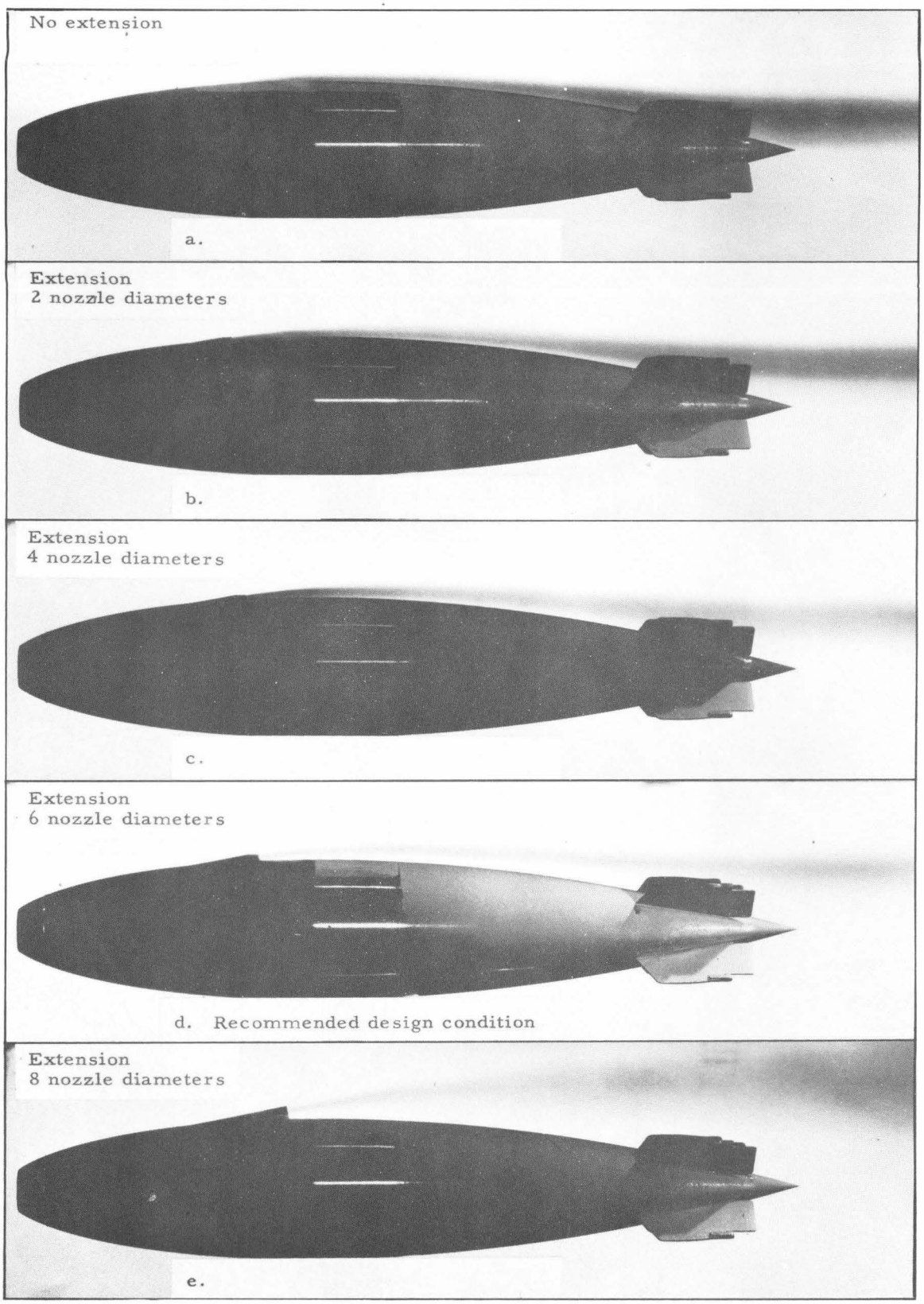

Fig. 13 - Photographs of Mk-40 model at operational jet-to-tunnel velocity ratio (U/V) of 2 showing effect of nozzle extension on scrubbing; tunnel velocity = 40 fps

extension and a very blunt nozzle extension, little effect on the scrubbing should result from improved nozzle exterior streamlining.

The effect of body turbulence on scrubbing was tested by the use of boundary layer trip wires and three differently finished afterbodies (Appendix). The results indicate that the model operates under turbulent conditions at all times.

Care should be taken in applying these results to the operational Mk-40 since all work was done without gas exhaust.

APPENDIX

Results of Tests with a Boundary Layer Trip Wire

Figure 14a shows the model without a trip wire at U/V = 1. Figure 14b shows the model with a trip wire operating under the same flow conditions. The wire can be seen near the front of the nose. Except for a slight difference in the intensity of the jet, there is no noticeable difference in the shape of the free jet or in the nature of the diffusion between the jet and the afterbody. This indicates that there is no trip wire effect. Since the model has a simulated nose duct only, there is no flow into this region. This causes the nose to act like a blunt nose, resulting in a turbulent boundary condition regardless of the use of a trip wire. Hence, all of the results contained herein are for a turbulent boundary condition.

Effect of Afterbody Finish on Scrubbing

Figure 15 shows the Mk-40 model with three different afterbody finishes operating under the same flow conditions. The upper picture shows an afterbody finished with a dichromate primer. The middle picture shows a dichromate finished model which has been carefully hand polished. The lower picture illustrates the model with an unfinished afterbody. The lower edge of the jet and the amount of diffusion towards the afterbody are the same in all three cases. This result is probably due to the fact that the blunt nose, as mentioned above, causes a turbulent boundary layer under all conditions. A later study will include tests with a smooth-nosed model to eliminate the inherent turbulent boundary layer.

Comparison of a Blunt and a Contoured Nozzle Extension Profile

Figure 16 illustrates the two types of nozzle extensions tested. The upper picture presents a contoured exterior nozzle profile, while the lower picture is of a blunt profile. There appears to be no difference between the two jets. These two profiles represent the worst and an average approach to the design of the exterior of this nozzle. Since the results presented here hold for both of these cases, it is reasonable to expect them to be valid for any smoothly designed nozzle extension which might be required by minimum drag considerations.

Reynolds Number Effect on Results

The Reynolds numbers noted in this report are based on model length and tunnel velocity. Figure 17 shows a jet at a U/V = 2 for Reynolds numbers from 1.6×10^6 to 4.0×10^6. There is no apparent difference among the three jets shown, indicating no Reynolds number effect in this range.

BIBLIOGRAPHY

1. Strumpf, A., "Analysis of the Effect of Hydrojets Upon Hydrodynamic Coefficients, Mark 40 Test Vehicle", Stevens Institute of Technology, March 1949.

2. Küchemann, D., "Jet Diffusion in Proximity of a Wall". NACA T.M. No. 1214, May 1949.

3. Albertson, M. L., Dai, Y. B., Jensen, R. A., Rouse, H., "Diffusion of Submerged Jets ". Reprinted from Transactions of American Society of Civil Engineers, Vol. 115, 1950, p. 639.

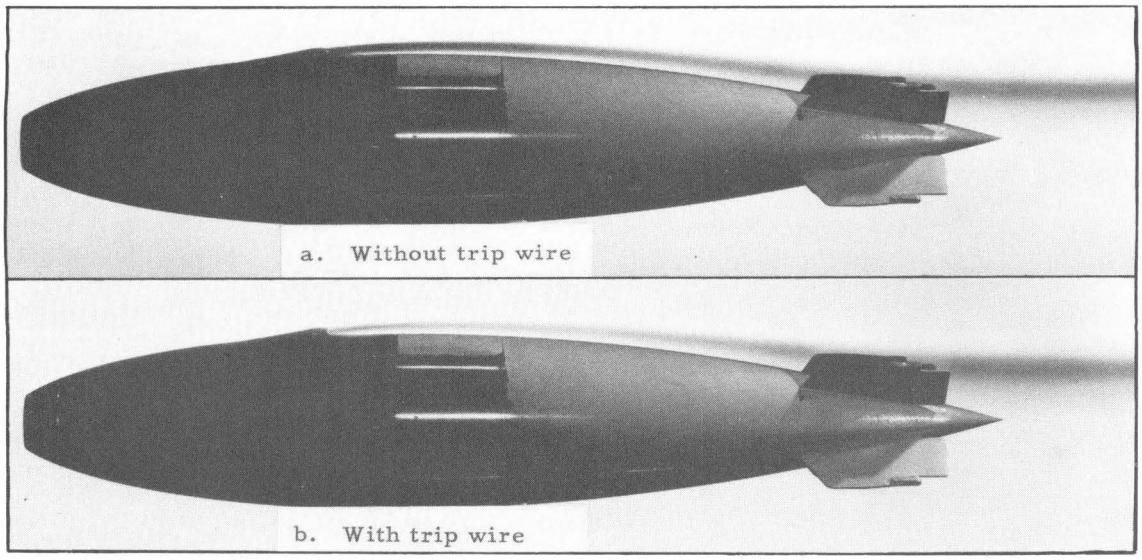

Fig. 14 - Effect of boundary layer trip wire on scrubbing.
U/V = 1 ; tunnel velocity = 40 fps

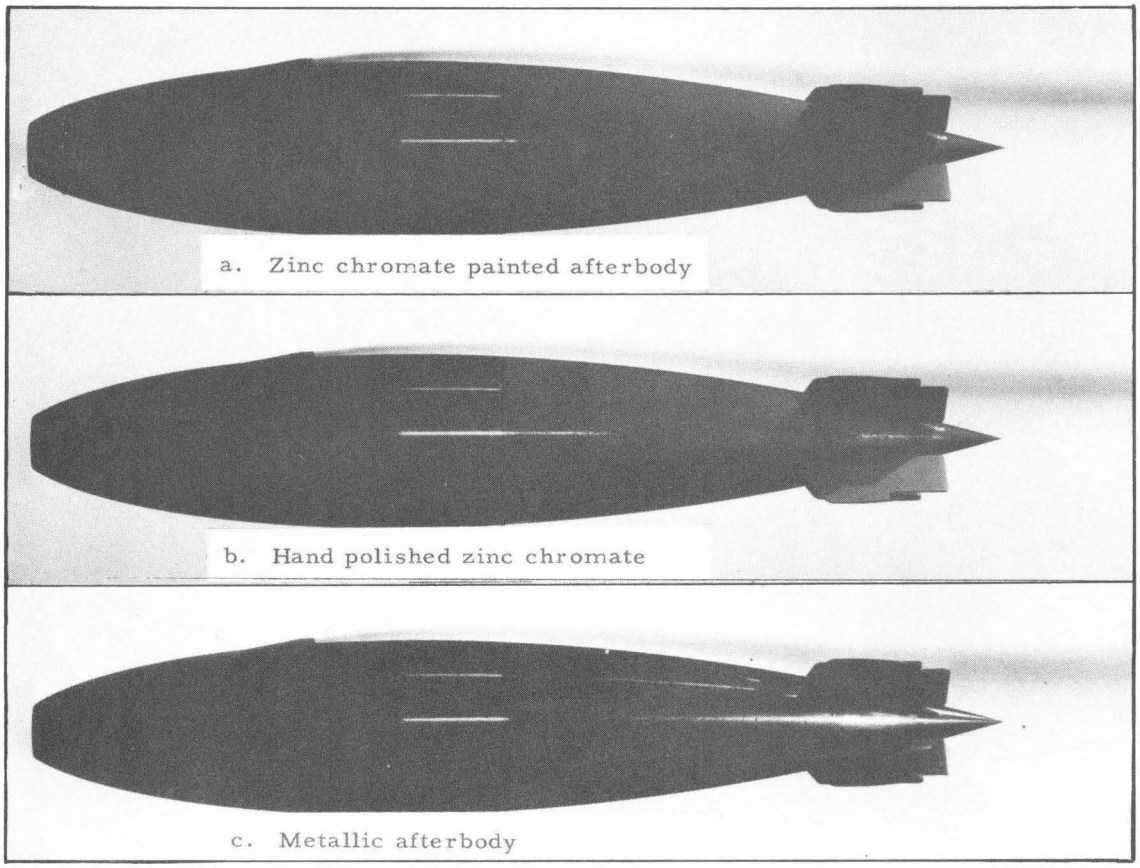

Fig. 15 - Effect of afterbody finish on scrubbing.
U/V = 1.5 ; tunnel velocity = 40 fps

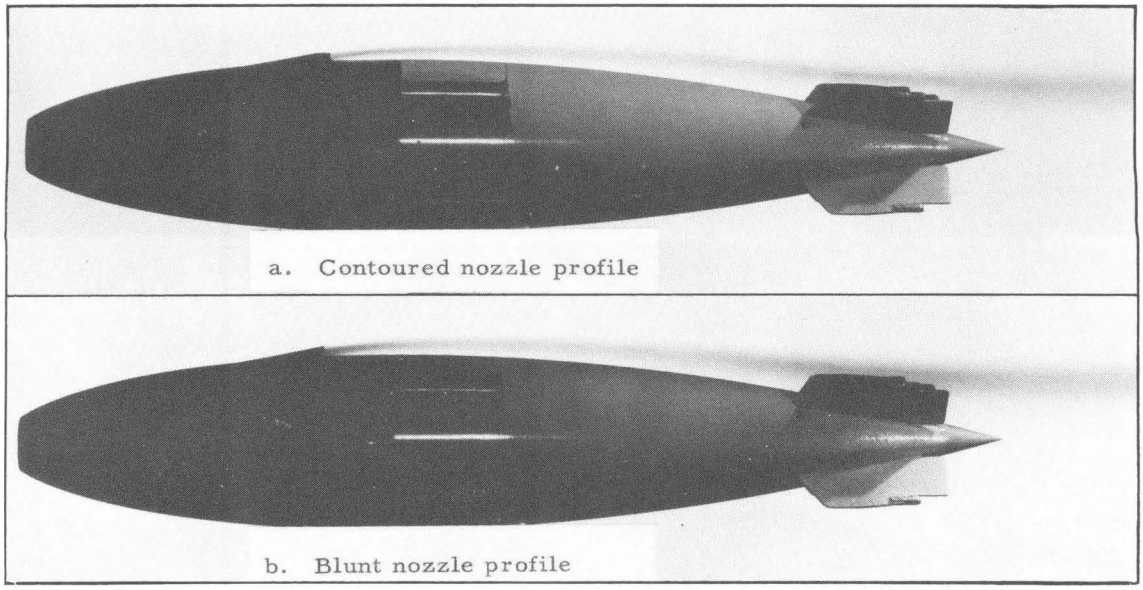

Fig. 16 - Effect of nozzle extension profile on scrubbing.
U/V = 1.5; tunnel velocity = 40 fps

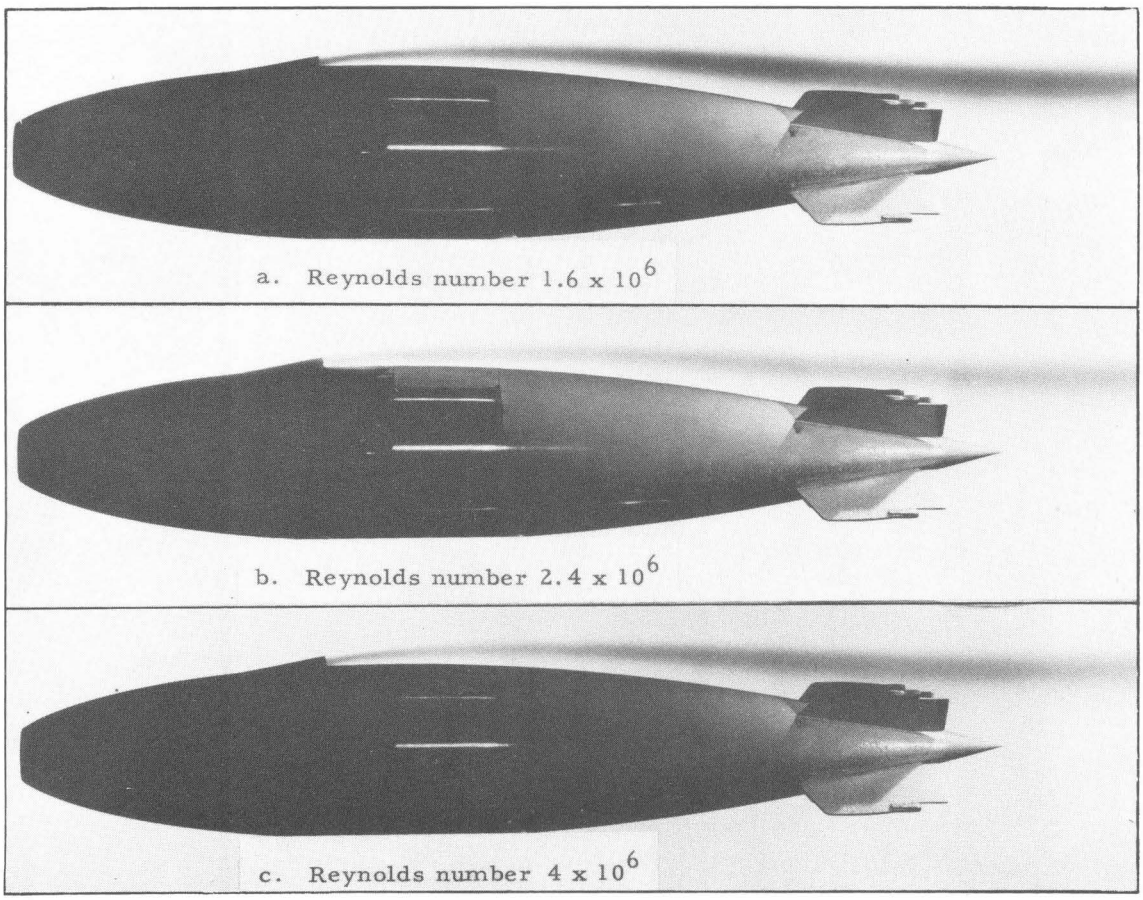

Fig. 17 - Effect of Reynolds number on scrubbing.
U/V = 2; nozzle extension 6 diameters

Department of the Navy
Bureau of Ordnance
Contract NOrd 9612

DISTRIBUTION LIST

Copy No.	
1	Chief, Bureau of Ordnance, Navy Dept., Washington, D.C. atten: Code Re6a
2	Chief, Bureau of Ordnance, Navy Dept., Washington, D.C. atten: Code Re3d
3-4	Chief, Bureau of Ordnance, Navy Dept., Washington, D.C. atten: Code Ad3
5-7	Chief, Bureau of Aeronautics, Navy Dept., Washington, D.C. atten: Code De3
8-12	Chief, Bureau of Ships, Navy Department, Washington 25, D.C.
13-15	Chief of the Office of Naval Research, Navy Dept., Washington, D.C., Code 438
16	Office of Naval Research, Los Angeles Branch, 1030 East Green Street, Pasadena, California
17-18	Director, David Taylor Model Basin, Washington 7, D.C.
19-20	Commanding Officer, Naval Torpedo Station, Newport, R.I.
21	Commander, Naval Ordnance Test Station, Inyokern, China Lake, California. Atten: Technical Library, Code 5507
22-23	Commander, Naval Ordnance Laboratory, White Oak, Silver Spring 19, Maryland
24-26	Officer-in-Charge, Pasadena Annex Naval Ordnance Test Station, Inyokern, 3202 East Foothill Blvd., Pasadena, California, atten: Pasadena Annex Library, Code P5507
27	Director, Experimental Towing Tank, Stevens Institute of Technology, via: Bureau of Aeronautics Representative, c/o Bendix Aviation Corp., Eclipse-Pioneer Division, Teterboro, New Jersey.
28	Director, Ordnance Research Laboratory, Pennsylvania State College, State College, Pennsylvania
29	Alden Hydraulic Laboratory, Worcester Polytechnic Institute, Worcester, Mass., via: Inspector of Naval Material, 495 Summer St., Boston 10, Mass.
30	Inspector of Naval Material, Development Contract Section, 1206 South Santee Street, Los Angeles, California
31-32	Superintendent, U.S. Navy Postgraduate School, Annapolis, Maryland.

Department of the Navy
Bureau of Ordnance
Contract NOrd 9612

Distribution List (Cont'd)

Copy No.	
33-34	Director, U.S. Naval Electronics Laboratory, Point Loma, San Diego, California
35-44	British Joint Services Mission, Navy Staff, via: Chief, Bureau of Ordnance, Navy Dept., Washington 25, D.C., atten: Code Ad8
45	Executive Secretary, Research and Development Board, National Defense Building, Washington, D.C.
46	Dr. E. Bromberg, Office of Naval Research, Mechanics Branch, Washington 25, D.C.
47	Commander, Submarine Development Group TWO, Box 70, U.S. Naval Submarine Base, New London, Conn.
48	Dr. F. C. Lindvall, 200 Throop, California Institute of Technology, Pasadena, California